Analyst

Accepted Manuscript

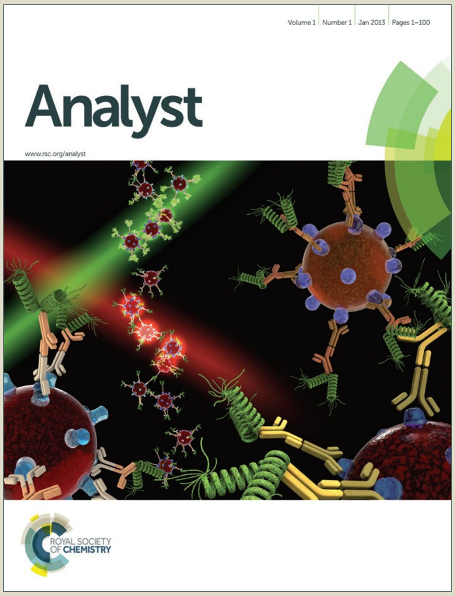
Volume 1 | Number 1 | Jan 2013 | Pages 1–100
Analyst
www.rsc.org/analyst
ROYAL SOCIETY OF CHEMISTRY

This is an *Accepted Manuscript*, which has been through the Royal Society of Chemistry peer review process and has been accepted for publication.

Accepted Manuscripts are published online shortly after acceptance, before technical editing, formatting and proof reading. Using this free service, authors can make their results available to the community, in citable form, before we publish the edited article. We will replace this *Accepted Manuscript* with the edited and formatted *Advance Article* as soon as it is available.

You can find more information about *Accepted Manuscripts* in the Information for Authors.

Please note that technical editing may introduce minor changes to the text and/or graphics, which may alter content. The journal's standard Terms & Conditions and the Ethical guidelines still apply. In no event shall the Royal Society of Chemistry be held responsible for any errors or omissions in this *Accepted Manuscript* or any consequences arising from the use of any information it contains.

ROYAL SOCIETY OF CHEMISTRY

www.rsc.org/analyst

Analyst RSCPublishing

ARTICLE

Cite this: DOI: 10.1039/x0xx00000x

Aqueous-filled polymer microcavity arrays: versatile & stable lipid bilayer platforms offering high lateral mobility to incorporated membrane proteins

Received 00th January 2012,
Accepted 00th January 2012

DOI: 10.1039/x0xx00000x

www.rsc.org/

Hajra Basit[a,§], Vinnie Gaul[a], Sean Maher[a], Robert J. Forster[a] and Tia E. Keyes[a] *

A key prerequisite in an ideal supported lipid bilayer based cell membrane model is that the mobility of both the lipid matrix and its components are unhindered by the underlying support. This is not trivial and with the exception of liposomes, many of even the most advanced approaches, although accomplishing lipid mobility, fail to achieve complete mobility of incorporated membrane proteins. This is addressed in a novel platform comprising lipid bilayers assembled over buffer-filled, arrays of spherical cap microcavities formed from microsphere template polydimethoxysilane. Prior to bilayer assembly the PDMS is rendered hydrophilic by plasma treatment and the lipid bilayer prepared using Langmuir Blodgett assembly followed by liposome/proteoliposome fusion. Fluorescence Lifetime Correlation Spectroscopy confirmed the pore suspended lipid bilayer exhibits diffusion coefficients comparable to free-standing vesicles in solution. The bilayer modified arrays are highly reproducible and stable over days. As the bilayers are suspended over deep aqueous reservoirs, reconstituted membrane proteins experience an aqueous interface at both membrane interfaces and attain full lateral mobility. Their utility as membrane protein platforms was exemplified in two case studies with proteins of different dimensions in their extracellular and cytoplasmic domains reconstituted into DOPC lipid bilayers; Glycophorin A, and Integrin $\alpha_{IIb}\beta_3$. In both cases, the proteins exhibited 100% mobility with high lateral diffusion coefficients.

Introduction

Membrane proteins (MPs) constitute nearly one third of all human proteins and are known to orchestrate key cellular functions ranging from ion transport,[1, 2] cell-cell attachment,[2] to signaling.[3] Consequently, such proteins are important targets in understanding disease progression and in pharmaceutical drug discovery. However, despite their importance, the direct *in vitro* study of membrane proteins lacks suitable high throughput screening membrane models, which can be reproducibly fabricated with controlled lipid composition, where the structural integrity and mobility of the protein is preserved upon reconstitution. A key feature of the cell membrane, vital to membrane protein function, is its inherent 2-D fluidity.[4, 5] Lateral diffusion of lipids and membrane proteins within the membrane regulate the distribution of membrane components and affect many processes, such as formation of protein complexes, which are involved in signaling and the dynamic assembly/disassembly of lipid disordered and ordered microdomains.[6]

Artificial models of biological membranes can provide enlightening insights into the behavior of membrane lipids and associated proteins by mimicking key facets of the cell membrane structure decoupled from the challenging complexity of the living cell. However, for an artificial bilayer model for support of membrane proteins to be credible, it must exhibit the property of high lateral mobility of both lipid and protein constituents. To this end, while Supported Lipid Bilayers (SLBs) are valuable artificial bilayer models, their inherent drawback is the interaction of the bilayer with the solid substrate, which dramatically lowers the mobility of the lipids and particularly incorporated membrane proteins compared with native cell membranes or free liposomes.[7-9] Key approaches to addressing this issue include Tethered Bilayer Lipid Membranes (t-BLMs) and Cushioned Bilayer Lipid Membranes. Although t-BLMs were shown to provide better stability to the lipid bilayers[10], diffusion coefficients of the lipids measured were not significantly improved compared to those measured for SLBs on planar substrates and the same is true for cushioned SLBs.[8, 11, 12] In order to obtain lipid bilayers that are sufficiently decoupled from the underlying substrates, another approach is to span lipid bilayers across nano sized apertures or pores, forming Black Lipid Membranes (BLM). BLMs however, suffer poor stability due to the retention of organic solvents that are commonly used in their preparation. Moreover, the incorporation and stability of membrane proteins is severely limited owing to their unfavorable mode of preparation and the remnant solvents within the bilayer.[13-15] Several groups have demonstrated elegant approaches to solvent free methods for pore-spanning lipid bilayers. However, most such techniques function in restricted conditions such as the limited (nano-dimensioned) size of the pores and the vesicles[16, 17], application of sheer flow and pH[18], the use of Giant Unilamellar Vesicles (GUVs)[14, 19] or spanning over dry substrates, where stability is a significant issue.[20-23] While each of these methods have shed light on the mechanisms of a variety of pore-spanning lipid membranes, the incorporation and manipulation of membrane proteins within artificial systems remains a challenge.

Herein, we describe a robust new supported lipid membrane model in which both lipid bilayer and reconstituted membrane proteins are highly mobile and evidently decoupled from the underlying substrate. The platform comprises lipid bilayers spanned over aqueous buffer-filled, micrometer sized hemispherical cavities formed from polystyrene sphere templated polydimethylsiloxane (PDMS) rendered hydrophilic by plasma treatment. We employ a combination of Langmuir-Blodgett and vesicle fusion techniques to obtain defect-free bilayers spanning the cavities. We demonstrate that the lipid bilayers can be reliably spanned across a range of cavity sizes prepared with templating spheres with diameters from 620 nm to 5 micrometers and that the spanning lipid bilayers remain intact, with reproducible fluidity over several days. This approach is facile, highly reproducible and importantly the cavity spanning lipid bilayer is assembled into a flow cell that can be directly mounted onto a microscope. The PDMS substrate lends itself to interference-free fluorescence studies even for, as demonstrated here, single molecule studies. Importantly, we demonstrate protocols for reconstitution of membrane proteins into these pore spanning lipid bilayers and demonstrate with two proteins with cytoplasmic or extracellular domains of different dimensions that they diffuse freely within the lipid over the pores, with 100% mobility and with diffusion coefficients comparable to those of the proteins reconstituted into liposomes.

Results and discussion

Fabrication of the microcavity arrays and spanning lipid bilayers

Figure 1, illustrates the key steps involved in preparing the polymer cavity array and preparing the bilayer. The PDMS cavity arrays were obtained by a modification of method previously described by us.[24] Briefly, PDMS was cast onto a dried film of polystyrene spheres, of the selected diameter, formed on mica, and cured. The spheres were removed to obtain open spherical cap cavities embedded in PDMS as described in detail in the Supporting Information. As described previously, this approach can be used to form extended and highly ordered 2 D arrays of microcavities, but as the focus of experiments here were at scale of tens of cavities, such arrays were not necessary and templating was restricted to small areas of the PDMS.[24]

As PDMS is hydrophobic, a critical step necessary to facilitate fluid filling and lipid membrane assembly is plasma treatment, which serves to render the substrate hydrophilic. This was reflected in the water droplet contact angle of 16^{o} measured for planar PDMS after plasma treatment. Following plasma treatment the cavities are then filled by sonication in buffer for 30 minutes, following which, a Langmuir layer of the phospholipid (containing the appropriate dye labeled DOPE) was spread over the filled cavity array, as described in the Supporting Information. The flow chamber as illustrated in Figure 1 is then constructed by adhering the edges of the hole-punched PDMS to a microscope cover slip using adhesive (SI for details). Phospholipid vesicles of the appropriate composition containing the dye with or without a reconstituted protein were then injected into the flow chamber to obtain the free-spanning lipid bilayers.

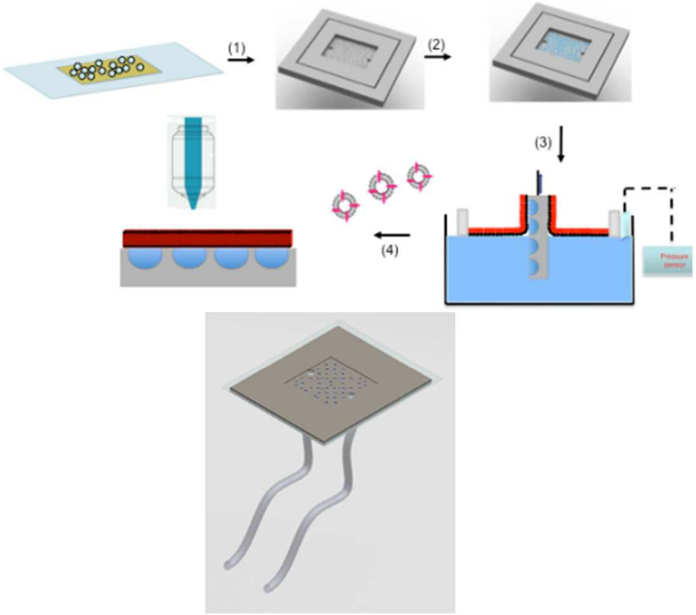

Figure 1. Top, Schematic illustration of the steps involved in the formation of free-spanning lipid bilayers over buffer-filled microcavities on PDMS. A dispersion of polystyrene spheres of selected diameter are drop casted onto a sheet of mica glued to glass and upon formation of a dry film spheres, PDMS is poured onto the glass and cured at 150 ºC. In step (1) the cured PDMS is peeled off and the spheres removed by treatment with THF. In step (2), the cavities were sonicated in buffer to facilitate their filling with buffer, followed by deposition of a lipid monolayer using Langmuir Blodgett technique (3). The bilayer is finally obtained by fusion of vesicles onto the deposited monolayer (4). Bottom Graphical representation of the filled cavity arrays on PDMS after their assembly in to a flow chamber.

Lipid bilayer spanned buffer-filled cavities

Lipid bilayer spanning across aqueous filled pores in PDMS with diameters of 602 nm, 1 μm, 2.94 μm and 5 μm were initially assessed using fluorescent confocal microscopy. Figure 2 presents the confocal images of the fluorescently doped DOPC bilayer spread on filled cavities labelled with 1 mol% of 1,2-dioleoyl-sn-glycero-3-phosphoethanolamine carboxyfluorescein. There is a significant refractive index difference between PDMS (n ≈1.45) and the buffer (n ≈1.33) and due to the spherical porous nature of the support the incident laser light scatters strongly at the positions of the filled cavities with the effect of making the buffer filled cavities look significantly brighter in the reflectance image than either the unfilled cavities or the planar regions of the PDMS platform, as shown in Figure 2 (a, c, e and g).

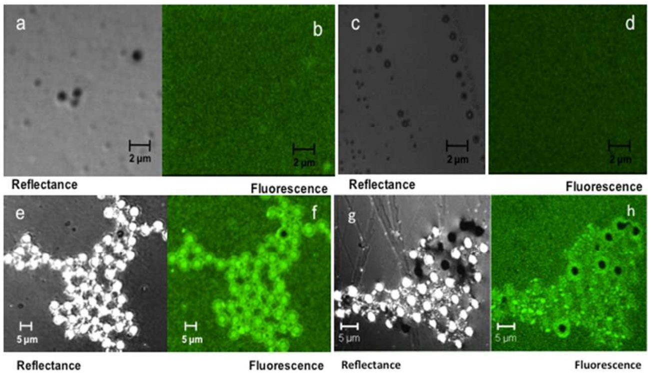

Figure 2. Confocal imaging upon pre-filling followed by bilayer formation using LB and vesicle fusion of cavities of sizes 620 nm (a & b), 1 μm (c & d), 2.94 μm (e & f) and 5 μm (g & h). Bilayers contained 1 mol% DOPE-Carboxyfluorescein as the fluorophore. The excitation wavelength was 488 nm. The fluorescence images (b, d, f and h) were collected using a 505 nm longpass filter, above 505 nm and reflectance images (a, c, e and g) were collected using a 420 nm longpass below 505 nm. Both fluorescence and reflectance images were collected simultaneously using two different channel.

This is a very useful characteristic that is exploited for accurately and precisely locating the pores with suspended bilayers.

It is evident from the reflectance images across all cavity diameters that not all cavities fill with buffer on sonication; typically 5 to 10% of cavities are unfilled. However, interestingly, the lipid bilayer was observed to span cavities whether they were buffer filled or not if the cavity diameter was 1μm or less. This is manifest in the confocal images shown in Figures 2b and 2d respectively, where the reflectance image demonstrates that a number of the cavities are unfilled but a homogenous fluorescence from top of the cavity indicates that the bilayer is spanning these apertures. In contrast, for the cavities exceeding 1 μm diameter i.e. those made from 2.94 μm and 5 μm spheres (Fig. 2f and 2h respectively), the bilayer was observed to span exclusively across buffer filled pores. When cavities of these dimensions were not pre-filled with aqueous solution, the lipid was observed to coat the interior surface of the array. Where this occurred, it was clear in microscopy, as each unfilled, lipid coated pore showed up as intense fluorescent spots. The aqueous support in the filled pores across which the Langmuir-Blodgett monolayer assembles, is required for formation of a spanning bilayer on the larger diameter cavities. Moreover, whereas the Langmuir-Blodgett technique is capable of forming homogenous monolayers over small defects (cavities), for the larger diameter un-filled cavities the LB films formed are discontinuous thus when the injected vesicles are introduced they form a bilayer in the interior walls of the cavity.

In order to assess the stability of the aqueous supported lipid bilayers across the cavities confocal fluorescence lifetime imaging was performed periodically on the supported bilayers across all the cavity sizes over a period of a week. The images showed that the lipid bilayers formed over filled cavities using the LB/vesicle fusion method were stable for a period of between 4-5 days, without significant alteration to fluidity. This extended stability, is a significant improvement on black lipid membranes or GUVs. Furthermore, the contacting solution at the external interface of the bilayer can be repeatedly washed without causing changes to its stability.

Fluidity of cavity supported lipid bilayers.

To assess the fluidity of cavity supported lipid bilayers we studied the lipid lateral diffusion coefficients of a DOPC bilayer at the arrays. The diffusion coefficient of lipid assembled over the cavity and at planar regions on the PDMS substrate were compared using Fluorescence Lifetime Correlation Spectroscopy (FLCS). The bilayers were labelled with a DOPE-Atto-655 dye at a concentration of 1 nM, which constitutes approximately a ratio of 1: 100,000 dye: lipid.[25] To accurately identify and distinguish the bilayer at the top planar regions of the array and bilayer suspended over the cavities for the FLCS experiment, both reflectance and fluorescence images were recorded, as described in Supporting Information. As described above and shown in Figure 3 (a) and (b), for a 2.94 μm diameter cavity array, the reflectance images are effective guides to locating filled-cavity spanning bilayers, and once found, z-scanning was used to locate the bilayer from optimal emission intensity. Autocorrelation functions (ACFs) were then recorded for bilayer at each (planar and cavity) surface region. The ACFs obtained were fit to the 2-dimensional model described in equation 1 to obtain the lateral diffusion co-efficient of DOPE-Atto655 in the bilayer.

$$G(\tau) = \frac{1}{N}\left[1+\left(\frac{\tau}{\tau_i}\right)^{\alpha}\right]^{-1} \qquad (1)$$

where, G(t) is the autocorrelation function, N is the average number of fluorescent molecules present in the confocal volume, τ_i is the characteristic residence time, and α is the anomalous parameter which reflects the extent of deviation of the diffusion from normal or Brownian motion where $\alpha = 1$[26], i is the index of the components. The lateral diffusion coefficient, D_L, can be obtained as $D_L = \omega^2 / 4\tau_i$, where, ω is the waist of the laser beam. To determine ω for each excitation, a reference solution of free dye was used for which the diffusion coefficient is known. For excitation at 640 nm, the reference dye was Atto-655 in water at 25 ^{o}C and its diffusion coefficient is 426 $\mu m^2\ s^{-1}$.[9, 27]

From FLCS, the diffusion co-efficient obtained for DOPE-Atto655 in the lipid bilayer supported over the planar region of the hydrophilic PDMS was found to be $4.1 \pm 0.6\ \mu m^2/s$ with α value of approximately 1 (i.e. = 0.997 ± 0.002). This value, was reproducible for all the PDMS substrates independent of their cavity sizes and is consistent with supported lipid bilayer diffusion previously reported on planar hydrophilic substrates.[9, 28]

In contrast, the lipid diffusion coefficient for the bilayer spanning across buffer filled cavities prepared from 2.94 μm diameter spheres was determined to be $10.2 \pm 0.6\ \mu m^2/s$ with an α value of 0.989 ± 0.004. Whereas, the diffusion coefficients of the bilayer spanning cavities made from 5 μm diameter spheres were determined to be $D = 11.2 \pm 0.4\ \mu m^2/s$ with α of 0.992 ± 0.002. i.e. within experimental error, the diffusion coefficients were approximately the same. The standard deviation on these values reflects replicates across 5 pores and 3 substrates of the same pore diameter. Interestingly though, the diffusion co-efficient values obtained from lipid bilayers spanning cavities made from 1 μm spheres was observed to be lower than those with larger pore diameters prepared from 2.94 µm and 5 µm diameter spheres at D = 7.1 ± 0.3 $\mu m^2/s$ and α at 1.012 ± 0.004.

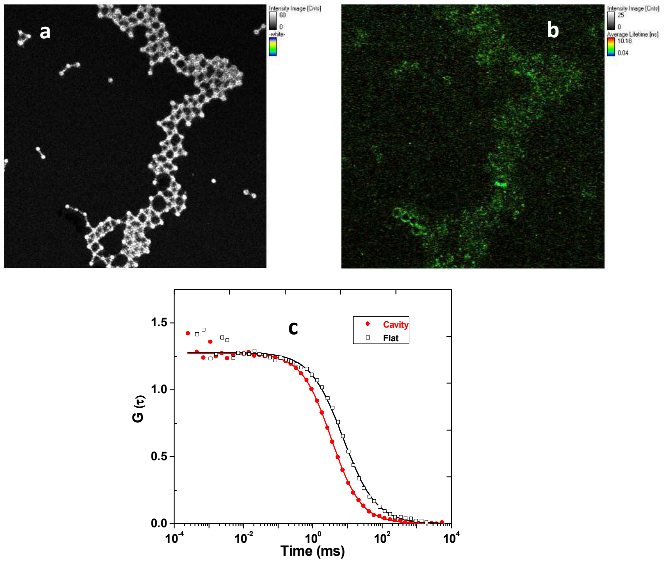

Figure 3. (a) reflectance and (b) FLIM images obtained for lipid spanning cavities made using 2.94 µm diameter spheres. The reflectance image allows for the identification of cavity points where FLCS should be performed. ATTO 655–DOPE at 1 nM concentration was used as the fluorophore and the image size is 80 µm × 80 µm. (c) Normalized autocorrelation function (ACF) curves measured above a single bilayer spanning cavity (red circular symbols) and on the flat regions of the supported bilayer (black rectangular symbols), measurements were acquired with 640 nm laser. The solid lines show the fits of the ACFs to equation (1).

This difference in diffusion coefficient may originate from differences in curvature of the lipid bilayer due to changes to the water meniscus, which will vary with cavity dimensions.[29] However, the key point to note here is the distinctly higher diffusion co-efficient values of the cavity spanning bilayers compared with lipid diffusion over planar PDMS regions (over 2 fold).

While, such diffusion values are consistent with those reported for lipids in GUVs in solution,[30] to the best of our knowledge this is the first report of such high fluidity in a supported bilayer system. The close resemblance of the diffusion value of the cavity spanning bilayer to that observed for GUVs indicates that the lipids spread over the cavity behave similarly to free-standing vesicles owing to the aqueous reservoir within the hemispherical pore below the inner leaflet of the spanning bilayer. As pore depth is estimated to approximately 65% the diameter of the pore, e.g. >1.9 µm for the 2.94 µm pore, the aqueous well is sufficiently deep, even for the smallest pores sizes, that there is little chance of protein or lipid over the pore interacting with the underlying substrate.

Diffusion studies of membrane proteins incorporate in the spanning bilayers

Motivated by the evident fluidity of the bilayers suspended over cavities, we next investigated the prospect of reconstituting membrane proteins into the cavity spanning lipid bilayers. For these studies, we employed the Human Glycophorin A (GpA) protein and platelet integrin $\alpha_{IIb}\beta_3$ as model proteins. These proteins were selected because of the diversity of their structure and particularly because of the large size of their extra-membrane components. GpA is one of the best-characterized membrane proteins, it is known to span the plasma membrane, with its C-terminal end at the cytoplasmic side of the membrane, a hydrophobic region penetrating through the membrane, and its N-terminal side, which is glycosylated, exposed to the exterior of the membrane.[31] GpA forms a symmetrical homodimer and has been shown to dimerize both in detergent micelles and in membranes owing to specific interactions between the TM helices.[32-35] The radius of the transmembrane dimer is reported to be 2.6 ± 0.4 nm.[36] In the present experiments, Glycophorin A was labelled with 5-Carboxytetramethylrhodamine (TAMRA) as described in the Supporting Information. The labeled GpA was reconstituted into DOPC vesicles labelled with DOPE-Atto 655 using the protocol described in the supporting information.[37]

The bilayer was formed by fusion of the labelled-GpA containing vesicles with DOPC monolayers formed over 2.94 µm template cavity substrates using LB deposition. As shown in Figure 4, the fluorescence lifetime image of the resulting cavity supported lipid bilayer shows homogenous fluorescence from the TAMRA labeled GpA. Imaging at Atto655 excitation wavelength i.e. 640 nm, confirmed that the lipid bilayer was also uniformly formed across the substrate (data not shown). These results indicate that GpA was well incorporated within the bilayer. Interestingly, and consistent with its incorporation into the bilayer, the GpA was found to be essentially immobile over the planar regions of the PDMS substrate. This is reflected by the photobleaching in the fluorescence intensity-time curve shown in Figure 4(d) obtained from point measurements of TAMRA-GpA in the bilayer over planar PDMS. Photobleaching of the GpA TAMRA label is attributed to lack of protein lateral mobility owing to the interaction of the cytoplasmic region of the protein with the underlying planar PDMS. Conversely, GpA was found to be 100% mobile over the cavities and its diffusion coefficient over the cavity aperture was determined to be 7.1 ± 0.6 $\mu m^2/s$ with α of 0.992 ± 0.005, obtained by fitting the FCS autocorrelation curve in figure 4(c) using equation 1. The lateral mobility is also seen in the intensity-time curve showing stable intensity fluctuations over the time of measurement (Figure S3). As expected the diffusion coefficient for the protein is considerably lower than the diffusion values for the lipid but is sufficiently high to indicate that GpA experiences little or no frictional interaction with the underlying surface.

In a previous report, the diffusion coefficient of GpA in free standing DMPC liposomes above its phase transition temperature was reported to be D_{GpA} = 4 ± 2 $\mu m^2/s$ using Fluorescence Recovery after Photobleaching (FRAP), whereas DMPC mobility was observed to be 5 ± 1.5 $\mu m^2/s$.[38] The ratio of Lipid to GpA diffusion coefficients are of the same order as that observed in our system. Such close lipid and membrane protein diffusions have so far only been observed in support free lipid bilayers such as vesicles and droplet hydrogel bilayers.[39]

The second model protein we examined was the platelet integrin protein $\alpha_{IIb}\beta_3$, which is a cell adhesion molecule consisting of a heterodimer of an alpha and beta subunit that spans the cytoplasmic membrane once. It has a large extracellular domain, (approx. 110 Å) and relatively smaller cytoplasmic tail (approx. 20 Å), though these dimensions depend on the activation status of the integrin.[40, 41] The Stokes radius of intact $\alpha_{IIb}\beta_3$ Integrin in dodecyl maltoside micelles in the presence of Ca^{2+}/Mg^{2+} was determined to be 6.95 ± 0.04 nm.[42] Previous studies of $\alpha_{IIb}\beta_3$ in artificial lipid systems have focused on glass supported bilayers or polymer cushioned bilayers with mobility and diffusion assessed from fluorescence recovery after photobleaching, FRAP.[43, 44] Erb et al reported a diffusion co-efficient of 0.70 ± 0.06 $\mu m^2/s$ for $\alpha_{IIb}\beta_3$ in a bilayer on glass.[43] Whereas Goennenwein et al. reported no fluorescence recovery on glass, but a diffusion co-efficient of 0.60 ± 0.2 $\mu m^2/s$ upon using a cellulose cushion.[44] In all reports, a large percentage of protein was deemed immobile. The reflectance, FLIM and FLCS studies of this protein incorporated into DOPC suspended across the 2.94 μm diameter arrays are shown in Figure 5.

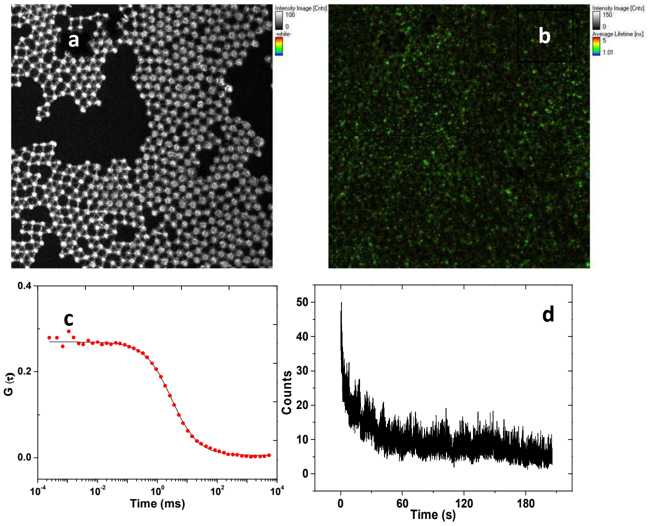

Figure 4. Reflectance (a) and (b) Fluorescence lifetime image of the Glycophorin A containing DOPC bilayer spanning a cavity made from 2.94 μm sized spheres. (c) Autocorrelation curves measured a single cavity (red circular symbols) from the arrays shown above, (d) Intensity-time curve for the measurement performed on the planar region of the array. Measurements were recorded over 300 s. In all experiments the only fluorophore is Glycophorin A which is labelled with the fluorophore TAMRA, the excitation wavelength is 532 nm.

Consistent with previous reports, extensive bleaching of the Integrin Atto-655 label was observed from the bilayer at the planar regions of the PDMS cavity array, where we found majority of the integrin to be immobile. However, $\alpha_{IIb}\beta_3$ reconstituted into cavity spanning bilayers over cavities prepared from 2.94 μm diameter spheres Figure 5(c), exhibited high mobility, with no evidence of photobleaching (Figure S4), and a diffusion co-efficient of 3.2 ± 0.33 $\mu m^2/s$ obtained from FLCS. Notably, the diffusion value correlates well with that reported for the same integrin in liposomes.[45] Crucially, no immobile fraction was identified indicating unencumbered lateral mobility of $\alpha_{IIb}\beta_3$ when incorporated into lipid over microcavity in this supported lipid bilayer system. Importantly, the diffusion coefficients measured for the two proteins are in good agreement with the theory suggested by Gambin et al., where they propose the lateral mobility of the membrane protein to be inversely proportional to its radius (D α 1/R) according to the following equation.[46]

$$D = \frac{k_B T \lambda}{4\pi\mu h R} \qquad (2)$$

Where, k_B is Boltzmann constant, T is absolute temperature, h is the thickness of the bilayer, μ is the viscosity of the membrane and λ is the characteristic length, a parameter included to satisfy dimensionality.

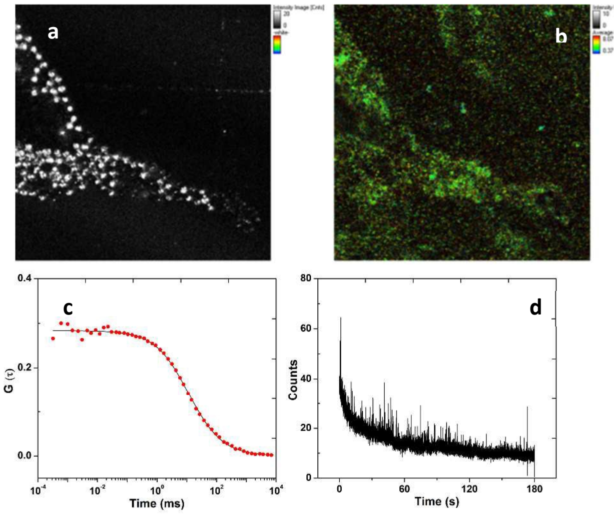

Figure 5. (a) Reflectance image of the PDMS substrate that allows for the location of buffer filled cavities. (b) Fluorescence lifetime image of Integrin $\alpha_{IIb}\beta_3$ labelled with ATTO 655 in a DOPC lipid bilayer above the cavities shown in a. Both images are 80 x 80 μm. FLCS point measurements were performed on the labeled protein on both planar PDMS and above cavities based on the reflectance image a. (c) Autocorrelation curve for integrin $\alpha_{IIb}\beta_3$ measured above a 2.94 μm spanning cavity (red circular symbols). (d) Intensity-time curve for the measurement performed over flat regions on the supported lipid bilayer. In both measurements, the fluorophore observed is integrin $\alpha_{IIb}\beta_3$ tagged with ATTO 655. Measurements were recorded over 180 s.

Since, the lipid composition was identical for both proteins studied, the viscosity of the bilayers can be considered to be identical. Thus upon correlating the diffusion co-efficients to their radii, we observe that D_{GpA}: $D_{\alpha IIb\beta 3}$ is nearly equal to $R_{\alpha IIb\beta 3}$: R_{GpA}, consistent with the theory suggested in Equation 2.

Conclusions

In summary, the results presented demonstrate that aqueous filled microcavity supported lipid bilayer arrays are potentially valuable tools for biophysical study of lipids and membrane proteins. The platforms have the versatility and stability of a supported lipid bilayer, with the fluidity of a liposome, due to the aqueous filled wells over which the bilayer is supported. A distinct feature of the described assembly is that there are no restrictions such as pH, solvent, and size of cavities or vesicles, sheer pressure etc. to obtain spanning lipid bilayers. The porous nature of the array offers the opportunity to vary solution at each side of the membrane. Lipid bilayer assembly onto hydrophilic PDMS substrates within a microfluidic chamber is not only extremely cost effective compared to other commonly used substrates such as Si_3N_4, SiO_2 or gold but also, because of the useful optical properties of PDMS, convenient to most microscopy platforms. In the present study we demonstrated a reliable methodology for incorporation of membrane proteins into the array, which should be broadly applicable across any membrane protein that can be reconstituted into liposomes. We demonstrated this method by incorporating two different membrane proteins into the array and confirmed high lateral mobility in both. This is a significant outcome as, currently apart from liposomes there are no effective artificial models for studying mobility of membrane proteins. Particularly important is the reconstitution of integrin into the layer as these proteins in particular require on high mobility in the cell membrane for their participating in signalling and protein recruitment so artificial models into which such proteins can be reconstituted retaining high mobility offer exciting opportunities to better understand their behaviour.

Overall, the presented platforms offer significant promise as rational chip-based cell bilayer models and they should be amenable to broad application from fundamental biophysical studies, to pharmaceutical drug discovery.

Acknowledgements

This material is based upon work supported by the Science Foundation Ireland under Grant No. [10/IN.1/B3025]. Lorcan Kent, DCU, is gratefully acknowledged for help with the drawings.

Notes and references

School of Chemical Sciences, National Centre for Sensor Research, Dublin City University, Dublin 9, Ireland. E-mail: tia.keyes@dcu.ie; Tel: +3531 7008185

§Current Affiliation: Chemistry Research Laboratory, University of Oxford.

†Electronic Supplementary Information (ESI) available: [Fabrication of microcavity arrays and spanning lipid bilayers, labelling of membrane proteins and their incorporation, confocal and FLIM imaging and FLCS data]. See DOI: 10.1039/b000000x/

1. F. M. Ashcroft, *Nature*, 2006, 440, 440-447.
2. S. J. Tucker, P. Tammaro and F. M. Ashcroft, *Ion channels and disease*, Academic press, 1999.
3. R. Juliano, *Annu. Rev. Pharmacool. Toxicol.*, 2002, 42, 283-323.
4. G. Espinosa, I. Lopez-Montero, F. Monroy and D. Langevin, *Proc. Natl. Acad. Sci. U. S. A.*, 2011, 108, 6008-6013.
5. D. Marguet, P.-F. Lenne, H. Rigneault and H.-T. He, *EMBO J.*, 2006, 25, 3446-3457.
6. J. E. Goose and M. S. P. Sansom, *PLoS Comput. Biol.*, 2013, 9.
7. M. Przybylo, J. Sýkora, J. Humpolíčková, A. Benda, A. Zan and M. Hof, *Langmuir*, 2006, 22, 9096-9099.
8. L. Zhang and S. Granick, *J. Chem. Phys.*, 2005, 123, 211104.
9. T. Tabarin, A. Martin, R. J. Forster and T. E. Keyes, *Soft Matter*, 2012, 8, 8743-8751.
10. H. Basit, A. Van der Heyden, C. Gondran, B. Nysten, P. Dumy and P. Labbe, *Langmuir*, 2011, 27, 14317-14328.
11. M. L. Wagner and L. K. Tamm, *Biophys. J.*, 2000, 79, 1400-1414.
12. C. Rossi, E. Briand, P. Parot, M. Odorico and J. Chopineau, *J. Phys. Chem. B*, 2007, 111, 7567-7576.
13. E. Reimhult and K. Kumar, *Trends Biotechnol.*, 2008, 26, 82-89.
14. E. K. Schmitt, M. Nurnabi, R. J. Bushby and C. Steinem, *Soft Matter*, 2008, 4, 250-253.
15. D. Weiskopf, E. K. Schmitt, M. H. Kluehr, S. K. Dertinger and C. Steinem, *Langmuir*, 2007, 23, 9134-9139.
16. K. Kumar, L. Isa, A. Egner, R. Schmidt, M. Textor and E. Reimhult, *Langmuir*, 2011, 27, 10920-10928.
17. H. Im, N. J. Wittenberg, A. Lesuffleur, N. C. Lindquist and S.-H. Oh, *Chemical Science*, 2010, 1, 688-696.
18. P. Jonsson, M. P. Jonsson and F. Hook, *Nano Lett.*, 2010, 10, 1900-1906.
19. S. Kresak, T. Hianik and R. L. C. Naumann, *Soft Matter*, 2009, 5, 4021-4032.
20. A. Simon, A. Girard-Egrot, F. Sauter, C. Pudda, N. P. D'Hahan, L. Blum, F. Chatelain and A. Fuchs, *J. Colloid Interface Sci.*, 2007, 308, 337-343.
21. M. R. Nussio, G. Oncins, I. Ridelis, E. Szili, J. G. Shapter, F. Sanz and N. H. Voelcker, *J. Phys. Chem. B*, 2009, 113, 10339-10347.
22. V. C. Stimberg, J. G. Bomer, I. van Uitert, A. van den Berg and S. Le Gac, *Small*, 2013, 9, 1076-1085.
23. C. Schmidt, M. Mayer and H. Vogel, *Angew. Chem. Int. Ed.*, 2000, 39, 3137-3140.
24. C. T. Mallon, R. J. Forster, and T. E. Keyes, *Chem. Commun.*, 2011, 47, 7605.
25. H. Basit, S. G. Lopez and T. E. Keyes, *Methods* 2014, 68, 286-299.
26. C. Favard, J. Wenger, P.-F. Lenne and H. Rigneault, *Biophys. J.*, 2011, 100, 1242-1251.
27. T. Dertinger, V. Pacheco, I. von der Hocht, R. Hartmann, I. Gregor and J. Enderlein, *ChemPhysChem*, 2007, 8, 433-443.
28. A. Benda, M. Beneš, V. Marecek, A. Lhotský, W. T. Hermens and M. Hof, *Langmuir*, 2003, 19, 4120-4126.
29. S.-C. J. Huang, A. B. Artyukhin, J. A. Martinez, D. J. Sirbuly, Y. Wang, J.-W. Ju, P. Stroeve and A. Noy, *Nano Lett.*, 2007, 7, 3355-3359.
30. F. Heinemann, V. Betaneli, F. A. Thomas and P. Schwille, *Langmuir*, 2012, 28, 13395-13404.
31. V. Anbazhagan and D. Schneider, *Biochim. Biophys. Acta, Biomembr.*, 2010, 1798, 1899-1907.
32. H. Furthmayr and V. Marchesi, *Biochemistry*, 1976, 15, 1137-1144.
33. M. A. Lemmon, J. M. Flanagan, H. R. Treutlein, J. Zhang and D. M. Engelman, *Biochemistry*, 1992, 31, 12719-12725.
34. K. R. MacKenzie, J. H. Prestegard and D. M. Engelman, *Science*, 1997, 276, 131-133.
35. L. E. Fisher, D. M. Engelman and J. N. Sturgis, *J. Mol. Biol.*, 1999, 293, 639-651.
36. K. Mineev, E. Bocharov, P. Volynsky, M. Goncharuk, E. Tkach, Y. S. Ermolyuk, A. Schulga, V. C. I. Maslennikov, R. Efremov and A. Arseniev, *Acta naturae*, 2011, 3, 90.
37. E. J. J. Vanzoelen, A. J. Verkleij, R. F. A. Zwaal and L. L. M. Vandeenen, *Eur. J. Biochem.*, 1978, 86, 539-546.
38. H. G. Kapitza, D. A. Ruppel, H. J. Galla and E. Sackmann, *Biophys. J.*, 1984, 45, 577-587.
39. J. R. Thompson, A. J. Heron, Y. Santoso and M. I. Wallace, *Nano Lett.*, 2007, 7, 3875-3878.
40. B. D. Adair and M. Yeager, *Proc. Natl. Acad. Sci.*, 2002, 99, 14059-14064.
41. J. Bennett, B. Berger and P. Billings, *J. Thromb. Haemost.*, 2009, 7, 200-205.
42. E. T. Eng, B. J. Smagghe, T. Walz and T. A. Springer, *J. Biol. Chem.*, 2011, 286, 35218-35226.
43. E. M. Erb, K. Tangemann, B. Bohrmann, B. Muller and J. Engel, *Biochemistry*, 1997, 36, 7395-7402.
44. S. Goennenwein, M. Tanaka, B. Hu, L. Moroder and E. Sackmann, *Biophys. J.*, 2003, 85, 646-655.
45. V. Gaul, S. G. Lopez, B. R. Lentz, N. Moran, R. J. Forster and T. E. Keyes, *Integrative Biology*, 2015, Advance Article, DOI: 10.1039/C1035IB00003C
46. Y. Gambin, R. Lopez-Esparza, M. Reffay, E. Sierecki, N. Gov, M. Genest, R. Hodges and W. Urbach, *Proc. Natl. Acad. Sci. U. S. A.*, 2006, 103, 2098-2102.